Thimerosal stimulates Ca^{2+} flux through inositol 1,4,5-trisphosphate receptor type 1, but not type 3, via modulation of an isoform-specific Ca^{2+}-dependent intramolecular interaction

Geert BULTYNCK[1], Karolina SZLUFCIK[1], Nael Nadif KASRI, Zerihun ASSEFA, Geert CALLEWAERT, Ludwig MISSIAEN, Jan B. PARYS and Humbert DE SMEDT[2]

Laboratorium voor Fysiologie, K.U.Leuven Campus Gasthuisberg O/N, Herestraat 49, B-3000 Leuven, Belgium

Thiol-reactive agents such as thimerosal have been shown to modulate the Ca^{2+}-flux properties of IP_3 (inositol 1,4,5-trisphosphate) receptor (IP_3R) via an as yet unidentified mechanism [Parys, Missiaen, De Smedt, Droogmans and Casteels (1993) Pflügers Arch. **424**, 516–522; Kaplin, Ferris, Voglmaier and Snyder (1994) J. Biol. Chem. **269**, 28972–28978; Missiaen, Taylor and Berridge (1992) J. Physiol. (Cambridge, U.K.) **455**, 623–640; Missiaen, Parys, Sienaert, Maes, Kunzelmann, Takahashi, Tanzawa and De Smedt (1998) J. Biol. Chem. **273**, 8983–8986]. In the present study, we show that thimerosal potentiated IICR (IP_3-induced Ca^{2+} release) and IP_3-binding activity of IP_3R1, expressed in triple IP_3R-knockout R23-11 cells derived from DT40 chicken B lymphoma cells, but not of IP_3R3 or $[\Delta 1–225]$-IP_3R1, which lacks the N-terminal suppressor domain. Using a $^{45}Ca^{2+}$-flux technique in permeabilized A7r5 smooth-muscle cells, we have shown that Ca^{2+} shifted the stimulatory effect of thimerosal on IICR to lower concentrations of thimerosal and thereby increased the extent of Ca^{2+} release. This suggests that Ca^{2+} and thimerosal synergetically regulate IP_3R1. Glutathione S-transferase pull-down experiments elucidated an interaction between amino acids 1–225 (suppressor domain) and amino acids 226–604 (IP_3-binding core) of IP_3R1, and this interaction was strengthened by both Ca^{2+} and thimerosal. In contrast, calmodulin and sCaBP-1 (short Ca^{2+}-binding protein-1), both having binding sites in the 1–225 region, weakened the interaction. This interaction was not found for IP_3R3, in agreement with the lack of functional stimulation of this isoform by thimerosal. The interaction between the IP_3-binding and transmembrane domains (amino acids 1–604 and 2170–2749 respectively) was not affected by thimerosal and Ca^{2+}, but it was significantly inhibited by IP_3 and adenophostin A. Our results demonstrate that thimerosal and Ca^{2+} induce isoform-specific conformational changes in the N-terminal part of IP_3R1, leading to the formation of a highly IP_3-sensitive Ca^{2+}-release channel.

Key words: Ca^{2+} signalling, intramolecular interaction, isoform-specific conformational change, *myo*-inositol 1,4,5-trisphosphate receptor, thiol-reactive agent, thimerosal.

INTRODUCTION

IP_3 (inositol 1,4,5-trisphosphate) receptors (IP_3Rs) are tetrameric intracellular Ca^{2+}-release channels, located in the endoplasmic reticulum of many mammalian cell types [1] and encoded by three different genes [2]. Each monomer can be divided into three regions: an N-terminal IP_3-binding domain, which is separated from the transmembrane C-terminal channel domain by a large internal coupling domain [2,3]. IP_3 binding to the N-terminal part of an IP_3R induces as yet unidentified intramolecular conformational changes in it and mediates subsequent opening of the C-terminal channel domain, followed by the release of Ca^{2+} from intracellular stores. Yoshikawa et al. [4] showed that IP_3Rs are composed of five stable trypsinolytic fragments and these fragments could still form a functional channel, indicating that they were kept together by intramolecular interactions. Very recently, Uchida et al. [5] described different IP_3R regions that are critical for the gating of the channel and pinpointed two essential, conserved cysteine residues in the C-terminal tail (Cys-2610 and Cys-2613) that are critical for IICR (IP_3-induced Ca^{2+} release).

Ca^{2+} exerts a bell-shaped activation of the IICR [6–9]. Low concentrations stimulate channel activity, whereas high concentrations have an inhibitory effect. Multiple Ca^{2+}-binding sites and a Ca^{2+}-sensor region have already been identified in the primary sequence of IP_3R1 [10–13]. Recently, it has been shown that Ca^{2+} significantly changes the conformation and molecular structure of purified IP_3R1. Ca^{2+} reversibly promotes transition from a square-shaped to a windmill-like structure, with relocation of the four peripheral IP_3-binding domains [14,15]. It was proposed that amino acids 651–1130, containing three possible Ca^{2+}-binding sites [11], may fulfil the function of a hinge region that drastically changes the conformation of the receptor after Ca^{2+} binding [5].

Thimerosal also has a bell-shaped effect on Ca^{2+} flux through IP_3R1 [16,17]. It increases the affinity of IP_3R2 for IP_3 in hepatocytes [18], whereas it has an inhibitory effect on Ca^{2+} flux through IP_3R3 [19]. However, effects of thimerosal on IICR are not always mimicked by identical effects on IP_3 binding [16,20]. The stimulatory effect of thimerosal on IP_3 binding to IP_3R1 from cerebellar microsomes [20] was also observed for the N-terminal IP_3-binding domain of the receptor (amino acids 1–581) [21], suggesting that thimerosal has critical interaction sites in this part of the protein. However, the exact molecular mechanism by which thimerosal specifically stimulates IP_3R1, but not IP_3R3 functioning, has not been elucidated.

In the present study, we have compared the functional and molecular effects of thimerosal on IP_3R1 and IP_3R3. We have assessed IICR in permeabilized A7r5 cells, where IP_3R1 is mainly expressed, and in R23-11 triple-knockout cells, which were

---

Abbreviations used: CaM, calmodulin; GST, glutathione S-transferase; IP_3, *myo*-inositol 1,4,5-trisphosphate; IICR, IP_3-induced Ca^{2+} release; IP_3R, IP_3 receptor; NEM, N-ethylmaleimide; sCaBP-1, short Ca^{2+}-binding protein-1.
[1] These authors contributed equally to this work.
[2] To whom correspondence should be addressed (e-mail Humbert.Desmedt@med.kuleuven.ac.be).

Table 1   PCR primer sequences for the construction of pGEX6p2 vectors containing amino acids 1–225, 226–604 and 1–604 of mouse IP$_3$R1 and rat IP$_3$R3

F, forward primer; R, reverse primer. See the text for details of the underlined regions.

Amino acids	Sequence	
	Mouse IP$_3$R1	Rat IP$_3$R3
1–225	F: TAACCGGATCCATGTCTGACAAAATGTCGAG	F: GCTATGAATTCCCATGAATGAAATGTCCAGCTTTCTTC
	R: CTCCCGAATTCTCATTTCATGAAAAGCACTATCTTC	R: GCCGTCACTCGAGTCACATGAATAAGTTGATCTTCCAGC
226–604	F: TAACCGGATCCTGGAGTGATAACAAAGACGAC	F: GCTATGAATTCCCCAGTTCCGGGACCATCTGGAG
	R: TTCCGAATTCTCATTTCCGGTTGTTGTGGAGCAGG	R: GCCGTCACTCGAGTCACTTCCGGTTGTTGTGCAGCAGG
1–604	F: TAACCGGATCCATGTCTGACAAAATGTCGAG	
	R: TTCCGAATTCTCATTTCCGGTTGTTGTGGAGCAGG	

originally derived from DT40 chicken B lymphoma cells, after the stable expression of one of these two isoforms. We have also analysed IP$_3$ binding to wild-type IP$_3$Rs and to a truncated IP$_3$R1 lacking its N-terminal 225 amino acids ([Δ1–225]-IP$_3$R1). We observed a co-ordinated effect of thimerosal and Ca^{2+} in stimulating IICR by IP$_3$R1, but not by IP$_3$R3. We found that the first 225 amino acids domain of IP$_3$R1, but not that of IP$_3$R3, directly interacted with the IP$_3$-binding core and this interaction was enhanced by both thimerosal and Ca^{2+}. In contrast, the inter-action between the N- and C-terminal parts of IP$_3$R1 was not affected by either thimerosal or Ca^{2+}, but was significantly in-hibited by IP$_3$ and adenophostin A. It is conceivable that the C-terminal channel domain via an IP$_3$-sensitive link can sense the Ca^{2+}- and thimerosal-evoked conformational changes in the N-terminal part of IP$_3$R1.

EXPERIMENTAL

Materials

Thimerosal and NEM (*N*-ethylmaleimide) were obtained from Sigma (St. Louis, MO, U.S.A.), [^{3}H]IP$_3$ from PerkinElmer (Boston, MA, U.S.A.), IP$_3$ from Roche (Penzberg, Germany), ^{45}Ca^{2+} from Amersham Biosciences (Uppsala, Sweden) and SIN-1 (3-morpholinosydnonimine/HCl) from EMD Biosciences (Darmstadt, Germany).

Cell culture

A7r5 embryonic rat aorta cells, obtained from A.T.C.C. (Bethesda, MD, U.S.A.) CRL 1444, and COS-1 SV40 African monkey kidney cells, obtained from A.T.C.C. CRL 1650, were cultured in Dulbecco's modified Eagle's medium, supplemented with 10 % (v/v) foetal calf serum, 3.8 mM L-glutamine, 0.9 % (v/v) non-essential amino acids, 85 i.u./ml penicillin, 85 μg/ml streptomycin and 20 mM Hepes (pH 7.4). All cell culture media and supplements were purchased from Invitrogen (Paisley, Renfrewshire, U.K.). A7r5 cells were seeded in 12-well plates (Costar, Corning, NY, U.S.A.) at a density of approx. 4×10^4 cells/ well. DT40 and R23-11 cell suspensions were cultured as des-cribed in [22]. R23-11 cells are IP$_3$R-knockout cells derived from DT40 chicken B lymphoma cells by homologous recombination and were kindly provided by Dr T. Kurosaki (Department of Mole-cular Genetics, Institute for Liver Research, Kansai Medical University, Moriguchi, Japan).

Plasmid vector constructs

For the construction of the vector encoding [Δ1–225]-IP$_3$R1, [pcDNA3.1(+) + mouse IP$_3$R1] was used as a template for the PCR, with forward primer 5′-TATGTCGCTAGCCTTAAGGCC-GCCATGTGGAGTGATAACAAAGACGAC-3′ and reverse pri-mer 5′-GGGAGAGGTACCAATTTTC-3′, and the amplified cDNA was cut with *Nhe*I and *Kpn*I (the respective restriction sites are underlined) and was ligated back into [pcDNA3.1(+) + mouse IP$_3$R1], which was also cut with *Nhe*I and *Kpn*I restriction enzymes.

For the construction of pGEX6p2 vectors (Amersham Bio-sciences) encoding amino acids 1–225, 226–604 and 1–604 of mouse IP$_3$R1, all coding regions were amplified by PCR from [pcDNA3.1(+) + mouse IP$_3$R1] used as a template. For the con-struction of pGEX6p2 vectors encoding the corresponding regions of rat IP$_3$R3, [pcDNA3.1(+) + rat IP$_3$R3] was used as a template. The sequences of the forward and reverse primers are listed in Table 1. The PCR products of IP$_3$R1 were digested with *Bam*HI and *Eco*RI (the respective restriction sites are underlined) and cloned into the *Bam*HI–*Eco*RI-treated pGEX6p2 vector. The PCR products of IP$_3$R3 were digested with *Eco*RI and *Xho*I (the respective restriction sites are underlined) and ligated into *Eco*RI–*Xho*I-treated pGEX6p2 vector.

For the construction of p3xFLAG-*myc*-CMV$^®$-24 expression vector (Sigma) encoding amino acids 2170–2749 [FLAG(2170–2749)] of mouse IP$_3$R1, [pcDNA3.1(+) + mouse IP$_3$R1] was used as a template for the PCR, with forward primer 5′-CAACAC-AAGCTTCAAACCATGCTGAAACCTGGAGG-3′ and reverse primer 5′-TACTGGATCCTTGGGCCGGCTGCTGTGGGTTG-ACATTC-3′. The PCR product of IP$_3$R1 was digested with *Hin*dIII and *Bam*HI (the respective restriction sites are underlined) and cloned into the *Hin*dIII–*Bam*HI-treated p3xFLAG-*myc*-CMV$^®$-24 expression vector.

All constructs were sequenced using the Automated Fluo-rescent$^®$ sequencing system (Amersham Biosciences).

Transfections

COS-1 cells were plated in 175 cm^2 dishes at 2.5×10^6 cells/dish, cultured for 24 h and transfected with 15–30 μg of DNA of FLAG (2170–2749) and 50 μl of FuGENE6$^®$ transfection reagent (Roche). Cells were harvested and/or analysed 72 h after trans-fection. R23-11 triple-knockout cells were transfected by electro-poration using a Gene Pulser apparatus (Bio-Rad). Briefly, approx. 10×10^6 cells in 0.5 ml of serum-free medium were transferred to a 4 mm electroporation cuvette (Eurogentec, Seraing, Belgium) and pulsed at 550 V and 25 μF in the presence of 100 μg of plas-mids. The electroporated cells were incubated in 30 ml of normal culture medium for 24 h before starting the selection with 1.5 mg/ ml G418 to generate stable cell lines.

Preparation of microsomes and determination of protein concentration

Total microsomes from R23-11 cells and from COS-1 cells trans-fected with FLAG(2170–2749) DNA construct were prepared

as described previously [23] and resuspended in 20 mM Tris/HCl (pH 7.4), 300 mM sucrose, 0.8 mM benzamidine and 0.2 mM PMSF. The microsomal preparations were stored at $-80\,^{\circ}\text{C}$. Protein concentration was determined by the method of Lowry et al. [24] after precipitation with 10 % (w/v) ice-cold trichloroacetic acid and using BSA as a standard. Protein concentration of the recombinant proteins was determined using the BCA (bicinchoninic acid) Protein Assay kit (Pierce Biotechnology, Rockford, IL, U.S.A.) according to the manufacturer's instructions.

[^{3}H]IP$_3$-binding assay

Binding studies were performed as described previously [25]. [^{3}H]IP$_3$ binding was performed at $0\,^{\circ}\text{C}$ by incubating samples in 160 μl of binding buffer containing 50 mM Tris/HCl (pH 8.3), 1 mM EDTA, 10 mM 2-mercaptoethanol and 10 nM [^{3}H]IP$_3$ for 30 min. In the experiments with NEM and thimerosal, protein samples were preincubated with the respective agent for 10 min at $0\,^{\circ}\text{C}$ before starting the binding assay, and the reducing agent 2-mercaptoethanol was omitted from the binding buffer. After incubation, the samples were rapidly passed through glass-fibre filters using a Combi cell harvester (Skatron, Lier, Norway). Non-specific binding was determined in the presence of 12.5 μM unlabelled IP$_3$. The amount of microsomes used was 200 μg.

SDS/PAGE and Western-blot analysis

Microsomes from different types of R23-11 cells were analysed by NuPAGE® 3–8 % (v/v) Tris/acetate SDS/polyacrylamide gels (Invitrogen); microsomes from COS-1 cells transfected with FLAG(2170–2749) by NuPAGE® 4–12 % (v/v) Bis-Tris SDS/polyacrylamide gels using Mops buffer (Invitrogen); GST (glutathione S-transferase) fusion proteins and amino acids 1–225 domains by NuPAGE® 4–12 % Bis-Tris SDS/polyacrylamide gels using Mes buffer (Invitrogen) according to the manufacturer's instructions. After semi-dry electrophoretic transfer on to a PVDF membrane (Immobilon-P; Millipore, Bedford, MA, U.S.A.) and blocking with PBS containing 1 % (v/v) Tween 20 and 5 % (w/v) non-fat dry milk powder, the blots were incubated first with the primary antibody and then with the alkaline phosphatase-conjugated secondary antibody. The immunoreactive bands were visualized after dephosphorylation of the Vistra® enhanced chemifluorescence substrate (Amersham Biosciences) and quantified using a Storm840 FluorImager equipped with ImageQuant 5.2 software (Molecular Dynamics, Sunnyvale, CA, U.S.A.). Statistical comparisons were performed by Student's t test. For immunodetection of the N-terminal regions of the IP$_3$R isoforms, we used the recently developed Rbt475 antibody (1:2500 to 1:3000). The epitope corresponds to amino acids 127–141 of the human IP$_3$R1, which are conserved in all the isoforms and across species; consequently, the antibody recognizes the various IP$_3$Rs having similar affinity ([26]; J. B. Parys, unpublished work). For the specific detection of IP$_3$R1, a polyclonal antibody Rbt03 (1:2500), whose epitope lies within residues 2735–2749, was used [27]. For immunodetection of FLAG(2170–2749) fusion protein, ANTI-FLAG® M2 monoclonal antibody (1:1500; Sigma) was used.

Purification of GST fusion proteins

For the preparation of GST fusion proteins, pGEX6p2 vectors containing the coding sequences for amino acids 1–225, 226–604 and 1–604 of mouse IP$_3$R1 and rat IP$_3$R3 were transformed into BL21(DE3) *Escherichia coli*. For GST–226–604 and GST–

1–604, colonies were grown overnight in 50 ml of Luria–Bertani medium at $30\,^{\circ}\text{C}$. Luria–Bertani medium (400 ml) was added to this pre-culture and bacteria were grown at $22\,^{\circ}\text{C}$ until the A_{600} reached 1.5. Addition of 0.1 mM isopropyl β-D-thiogalactoside to the bacterial culture, which was further grown at $14\,^{\circ}\text{C}$ for another 20 h, induced protein expression. Expression of 1–225 recombinant proteins was performed as described previously [11]. All proteins were further purified as described previously [11]. For amino acids 1–225, after washing the beads, the immobilized GST fusion proteins were treated for 2 h at $4\,^{\circ}\text{C}$ with PreScission Protease (40 units; Amersham Biosciences) in cleavage buffer (50 mM Tris/HCl, pH 7.0/150 mM NaCl/1 mM EDTA/1 mM dithiothreitol). All the purified proteins were dialysed overnight against PBS using Slide-A-Lyzer with a cut-off of 10 kDa (Pierce Biotechnology) and stored at $-80\,^{\circ}\text{C}$.

GST-pull-down assay

A GST-pull-down assay was performed by using the Profound Pull-Down GST protein–protein interaction kit (Pierce Biotechnology). Dialysed, purified GST–226–604 fusion proteins or parental GST (control) were immobilized on 50 μl of glutathione–Sepharose 4B (50 %) by incubation for 2 h at $4\,^{\circ}\text{C}$ in incubation buffer, i.e. 1 part TBS [20 mM Tris/HCl (pH 7.2)/ 150 mM NaCl] mixed with 1 part of ProFound® bacterial lysis buffer (Pierce Biotechnology) and supplemented with 1 mM 2-mercaptoethanol. After the GST fusion proteins were bound, the beads were washed twice with 500 μl of incubation buffer supplemented with 2-mercaptoethanol (1 mM) and twice with 500 μl of incubation buffer supplemented with either 2-mercaptoethanol (1 mM), thimerosal (100 μM) or NEM (300 μM) depending on the conditions. Purified 1–225 proteins were incubated with immobilized GST–226–604 for 2 h at $4\,^{\circ}\text{C}$ in incubation buffer, supplemented with 1 mM 2-mercaptoethanol, 100 μM thimerosal or 300 μM NEM. Unbound 1–225 protein was removed by washing the beads four times with 500 μl of the respective incubation buffer. Bound 1–225 proteins were eluted by incubating the beads with LDS® (Invitrogen) for 10 min at $70\,^{\circ}\text{C}$ and collected by centrifuging at 20000 g for 1 min at room temperature ($25\,^{\circ}\text{C}$).

Pull-down assay of FLAG(2170–2749) with GST–1–604

A GST-pull-down assay was performed by using the Profound Pull-Down GST protein–protein interaction kit (Pierce Biotechnology). Dialysed, purified GST–1–604 type 1 fusion proteins or parental GST (control) were immobilized on 50 μl of glutathione–Sepharose 4B (50 %) by incubation for 2 h at $4\,^{\circ}\text{C}$ in incubation buffer, i.e. 1 part of PBS without Ca^{2+} and Mg^{2+} buffer containing 0.8 mM benzamidine, 0.2 mM PMSF and 1 μg/ ml leupeptin mixed with 1 part of bacterial lysis buffer® (Pierce Biotechnology) and supplemented with 1 mM 2-mercaptoethanol. After the GST fusion proteins were bound, the beads were washed twice with 500 μl of incubation buffer supplemented with 2-mercaptoethanol (1 mM) and twice with 500 μl of incubation buffer supplemented with either 2-mercaptoethanol (1 mM) or thimerosal (100 μM) and EGTA (1 mM), Ca^{2+} (25 μM), IP$_3$ (20 μM) or adenophostin A (20 μM) depending on the conditions. COS-1 microsomes, originating from cells transfected with FLAG(2170–2749), were first solubilized by incubation for 2 h at $4\,^{\circ}\text{C}$ in 400 μl of PBS without Ca^{2+} and Mg^{2+} buffer containing 1 % Triton X-100, 0.8 mM benzamidine, 0.2 mM PMSF, 1 μg/ml leupeptin, 1 μg/ml aprotinin, 1 μg/ml pepstatin A and 0.5 μM NaCl and centrifuged at 125000 g for 25 min. Solubilized FLAG(2170–2749) protein was incubated with immobilized

GST–1–604 for 2 h at 4 °C in the corresponding incubation buffer. Unbound FLAG(2170–2749) was removed by washing the beads four times with 500 μl of PBS without Ca^{2+} and Mg^{2+} buffer containing 0.25 % Triton X-100, 0.8 mM benzamidine, 0.2 mM PMSF, 1 μg/ml leupeptin, supplemented with either 2-mercaptoethanol (1 mM) or thimerosal (100 μM) and EGTA (1 mM), Ca^{2+} (25 μM), IP$_3$ (20 μM) or adenophostin A (20 μM) depending on the conditions. Bound FLAG(2170–2749) proteins were eluted by incubating the beads with LDS® (Invitrogen) for 10 min at 70 °C and collected after centrifuging at 20 000 *g* for 1 min.

Ca^{2+}-release studies in permeabilized R23-11 and A7r5 cells

R23-11 cell pellets were resuspended in intracellular medium (120 mM KCl/30 mM Hepes, pH 7.4/1 mM MgCl$_2$) in the presence of 1 mM ATP, 25 mM phosphocreatine, 50 i.u. of creatine kinase and 5 μM fluo-3 (Molecular Probes, Eugene, OR, U.S.A.) and transferred to a 4 ml fluorescence quartz cuvette thermostatically maintained at 37 °C. Cell density was 5×10^7 cells/ml. Mild treatment of the cells with digitonin (50 μM) disrupted the plasma membrane. The fluo-3 fluorescence ($\lambda_{ex} = 503$ nm and $\lambda_{em} = 530$ nm) was measured with an Aminco–Bowman® Series 2 spectrometer (Spectronic Unicam, Rochester, NY, U.S.A.). A23187 (8 μM; Sigma) was added at the end of each experiment to measure the total releasable Ca^{2+}. This value varied slightly but not significantly in different cell batches due to the time of storage of the cells on ice after pelleting. The fluorescence signal F was calibrated by first adding 0.5 mM Ca^{2+} (F_{max}) and then adding 5 mM EGTA (F_{min}). The free [Ca^{2+}] was calculated using the equation $[Ca^{2+}] = K_d \cdot (F - F_{min})/(F_{max} - F)$ [28], with a dissociation constant K_d of 864 nM, as determined in the cytosol-like medium at 37 °C [29]. ^{45}Ca^{2+} fluxes on monolayers of saponin-permeabilized A7r5 cells at 25 °C were measured exactly as described previously [30].

RESULTS

Expression and characterization of wild-type IP$_3$R1, wild-type IP$_3$R3 and [Δ1–225]-IP$_3$R1 in IP$_3$R-knockout R23-11 cells

We stably expressed wild-type mouse IP$_3$R1, wild-type rat IP$_3$R3 and the deletion mutant of the mouse IP$_3$R1 lacking its first 225 amino acids ([Δ1–225]-IP$_3$R1) in R23-11 triple-knockout cells originating from DT40 chicken B lymphoma cells. Figure 1 shows a Western-blot analysis of the microsomal preparations from these stable cell lines together with the original DT40 cells using the polyclonal anti-IP$_3$R1 Rbt03 antibody (Figure 1A) and anti-IP$_3$R Rbt475 (Figure 1B). No IP$_3$R expression was detected in R23-11 cells. The immunoreactive band in the DT40 cells corresponds to the endogenous peripheral IP$_3$R1, which migrates faster than the heterologously expressed neuronal IP$_3$R1 (Figure 1A, second and third lanes). The broad band detected in DT40 cells with Rbt475 (Figure 1B) corresponds to the sum of the endogenous IP$_3$Rs.

IP$_3$-binding activities of the wild-type IP$_3$R1 and [Δ1–225]-IP$_3$R1 were measured by equilibrium [^{3}H]IP$_3$-binding analysis with 10 nM [^{3}H]IP$_3$. After subtraction of background [^{3}H]IP$_3$ binding to the membranes of the R23-11 cells, we found that [Δ1–225]-IP$_3$R1 bound approx. 7-fold more IP$_3$ when compared with the wild-type IP$_3$R1 (results not shown). This is compatible with previous studies reporting that a mutant IP$_3$R1 lacking the first 223 amino acids exhibited a 10-fold higher affinity for IP$_3$ when compared with the wild-type channel [5].

We then analysed the Ca^{2+}-release activity of the truncated channel in digitonin-permeabilized R23-11 cells. Wild-type
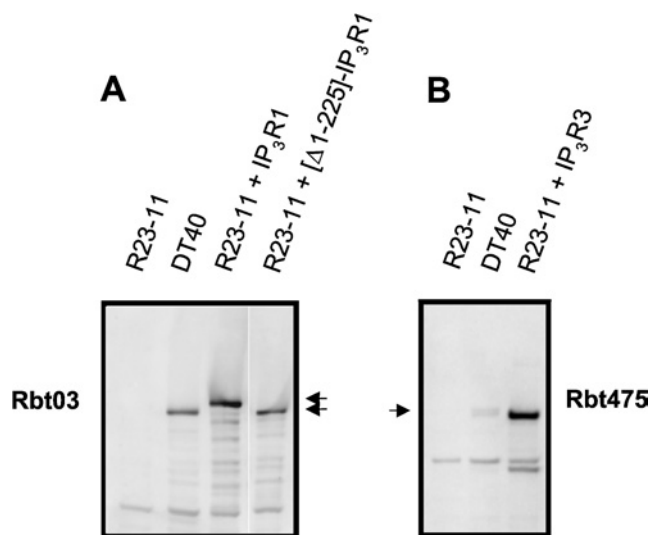

Figure 1   Expression of IP$_3$Rs in R23-11 cells

Microsomes (10 μg) from different R23-11 cell lines were separated on SDS/polyacrylamide gels and analysed by immunoblotting. The blot in (**A**) was probed with the anti-IP$_3$R1 polyclonal antibody Rbt03, whose epitope lies within residues 2735–2749, and the blot in (**B**) was probed with the anti-IP$_3$R polyclonal antibody Rbt475, whose epitope corresponds to the conserved stretch of amino acids in the N-terminus of all IP$_3$R isoforms. The arrows indicate the positions of the full-size IP$_3$Rs.

IP$_3$R1 exhibited a strong Ca^{2+} release after the addition of IP$_3$. In contrast, [Δ1–225]-IP$_3$R1 did not respond to (up to 25 μM) IP$_3$ (results not shown). Similarly, adenophostin A, a more potent and stable activator of IP$_3$R, induced a long-lasting increase in the free [Ca^{2+}] in cells heterologously expressing wild-type IP$_3$R1 (Figure 2A), but had no effect on [Δ1–225]-IP$_3$R1-expressing cells (Figure 2B). These findings are compatible with the other studies showing that the N-terminal 225 amino acids fragment is critical for the functional activation of IP$_3$R [5].

Effect of thiol-reactive agents on IP$_3$ binding and IICR

We next examined the effect of thiol-reactive agents on IP$_3$-binding and Ca^{2+}-release properties of the wild-type IP$_3$R1 and [Δ1–225]-IP$_3$R1. In addition, we also examined the effect on wild-type IP$_3$R3, which was not stimulated by thimerosal [19–21]. We found that both thimerosal (100 μM), which catalyses the oxidation of thiol groups leading to the formation of S-S bridges, and NEM (300 μM), a thiol-alkylating agent, stimulated IP$_3$ binding to the wild-type IP$_3$R1 by approx. 2-fold (Figure 3A). Interestingly, the stimulatory effect of thimerosal and NEM on IP$_3$ binding was completely abolished in the cell line heterologously expressing [Δ1–225]-IP$_3$R1, indicating that the stimulatory effects of thimerosal and NEM on IP$_3$ binding may involve cysteine residues in the first 225 amino acids. In agreement with previous studies [20,21], IP$_3$ binding to the full-size IP$_3$R3 was stimulated neither by incubation with thimerosal nor by incubation with NEM (Figure 3A).

We observed that the preincubation with thimerosal enhanced IICR and rendered the subthreshold IP$_3$ concentration of 10 nM effective to release Ca^{2+} through the wild-type IP$_3$R1. This is demonstrated in Figure 3(B), where the free [Ca^{2+}] is shown as a function of time in permeabilized R23-11 cells heterologously expressing the wild-type IP$_3$R1. After preincubation with 100 μM thimerosal for approx. 5 min, the same concentration of IP$_3$ provoked significant Ca^{2+} release. When water was added instead of
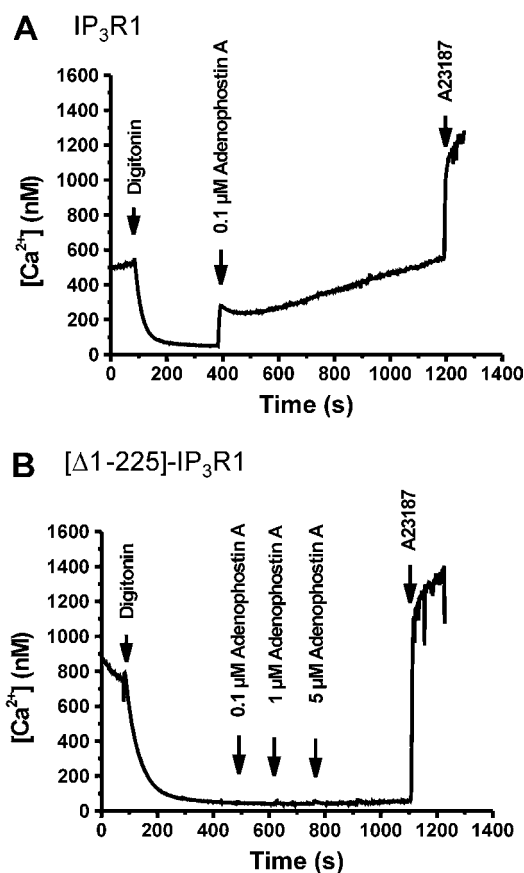
Figure 2 Ca²⁺-release properties in permeabilized R23-11 cells heterologously expressing IP₃R1 (A) and [Δ1–225]-IP₃R1 (B)

Free $[Ca^{2+}]$ was measured using fluo-3 fluorescence. After permeabilization of the plasma membrane with 50 μM digitonin, the cells accumulated Ca^{2+} in their intracellular stores, resulting in a decrease in medium-free $[Ca^{2+}]$. After stabilization of the signal, adenophostin A (concentrations are shown in the Figures) was added. At the end of each experiment, 8 μM A23187 was added to estimate the total releasable amount of Ca^{2+}. Results are typical for four independent experiments.

thimerosal, 10 nM IP₃ was still unable to induce Ca²⁺ mobilization (results not shown), indicating that the release induced by the second addition of IP₃ (10 nM) was due to thimerosal-mediated sensitization of IP₃R1. Furthermore, when a reducing agent such as 2-mercaptoethanol (1 mM) was used instead of thimerosal, 10 nM IP₃ did not provoke any measurable Ca²⁺-release activity and preincubation with 2-mercaptoethanol completely abolished the potentiating effect of thimerosal on IICR (results not shown). NEM, which augmented IP₃ binding to the same extent as thimerosal, did not enhance Ca²⁺ flux through IP₃R1 (Figure 3E). At a total concentration of 300 μM, NEM inhibits the Ca²⁺-uptake activity of the SERCA (sarcoplasmic/endoplasmic-reticulum Ca²⁺-ATPase) pumps, explaining the increase in the basal Ca²⁺ levels. This suggests that the oxidizing effect of thimerosal is essential for the stimulatory action and that alkylation of cysteine residues by NEM is unable to mimic the effect of thimerosal. We propose that thimerosal catalyses the formation of S–S bridges between different parts of IP₃R1 and thereby influences the conformation.

The same experiment was performed for [Δ1–225]-IP₃R1 and IP₃R3. Thimerosal could neither render the truncated receptor active nor sensitize it to IP₃ (Figure 3C). A similar observation was obtained for IP₃R3, since up to 100 μM thimerosal could not potentiate IICR mediated by this isoform (Figure 3D). Moreover,
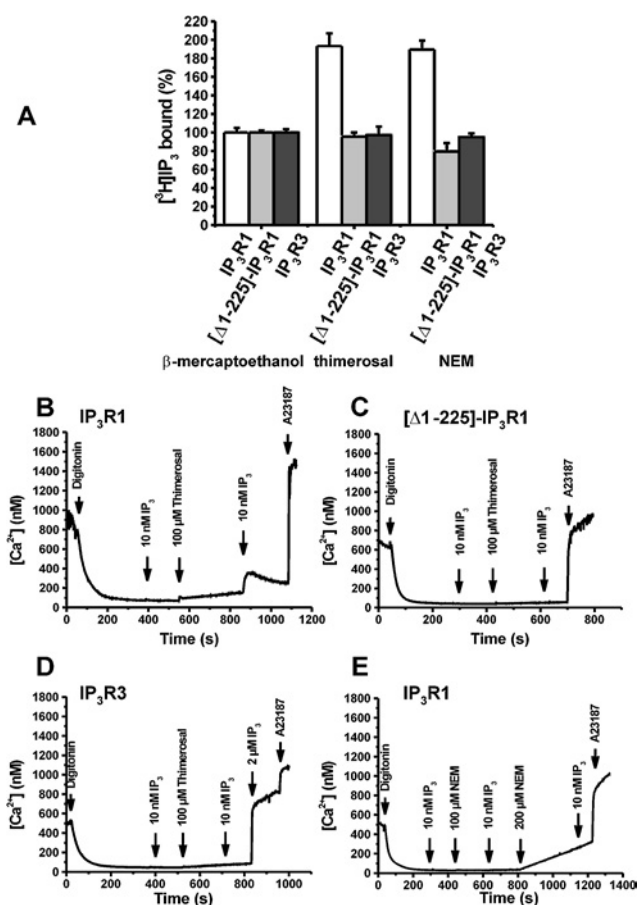

Figure 3 Effects of thimerosal and NEM on IP₃ binding and IICR in R23-11 cells heterologously expressing IP₃R1, [Δ1–225]-IP₃R1 and IP₃R3

(**A**) [³H]IP₃-binding assay performed on 200 μg of microsomes in a binding buffer at pH 8.3 using 10 nM [³H]IP₃ in the presence of 100 μM thimerosal or 300 μM NEM. Binding in the presence of 1 mM 2-mercaptoethanol was used as the control value (100 %). Results are expressed as the means $\pm$ S.E.M. for three independent experiments each performed in triplicate. (**B–D**) The effect of 100 μM thimerosal on IICR in permeabilized R23-11 cells heterologously expressing IP₃R1 (**B**), [Δ1–225]-IP₃R1 (**C**) and IP₃R3 (**D**). The experimental procedure was the same as that described in Figures 2(A) and 2(B). In these experiments, a subthreshold concentration of IP₃ (10 nM), which cannot provoke Ca²⁺ release, was used. After incubation with 100 μM thimerosal for 5 min, the same concentration of IP₃ (10 nM) was added. (**E**) The effect of 100 and 200 μM NEM on IICR in permeabilized R23-11 cells heterologously expressing IP₃R1. Results are typical for four independent experiments.

at higher IP₃ concentrations, there was no potentiation of IICR by 100 μM thimerosal (results not shown; [18]). The finding that thimerosal specifically exerts its activatory function on IP₃R1, but not on IP₃R3, suggests that thimerosal affects the cysteine residues that are not conserved between IP₃R1 and IP₃R3.

Effect of thimerosal and Ca²⁺ on IICR in permeabilized A7r5 cells

In A7r5 smooth-muscle cells, which mainly express IP₃R1, a biphasic effect of thimerosal on IICR was found [16]. We now found that Ca²⁺ modulated this biphasic effect of thimerosal on IICR. Figures 4(A) and 4(B) illustrate the fractional loss (the amount of Ca²⁺ leaving the stores within 2 min divided by the total store Ca²⁺ content at that time) as a function of time. The non-mitochondrial Ca²⁺ stores of permeabilized A7r5 cells, loaded to steady state with ⁴⁵Ca²⁺, slowly lost their accumulated Ca²⁺. Thimerosal (1 μM) strongly potentiated IICR and this was additive to the potentiation by Ca²⁺ (Figures 4A and 4B). A
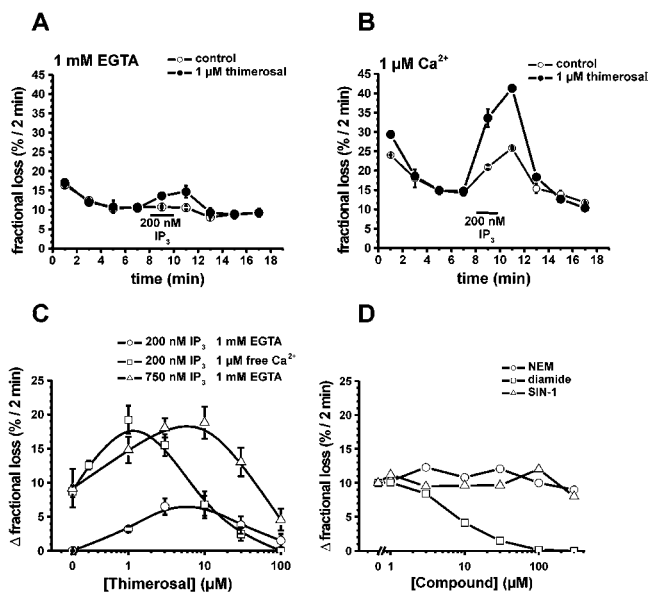
Figure 4   Effect of thimerosal on IICR in the presence or absence of 1 μM free Ca^{2+} in permeabilized A7r5 cells

Data are plotted as fractional loss (the amount of ^{45}Ca^{2+} leaving the stores in 2 min divided by the total store Ca^{2+} content at that time) as a function of time in (**A**, **B**). (**A**) Effect of the presence ($\bullet$) or absence ($\bigcirc$) of 1 μM thimerosal on Ca^{2+} release provoked by 200 nM IP$_3$ in the absence of Ca^{2+}. (**B**) Effect of the presence ($\bullet$) or absence ($\bigcirc$) of 1 μM thimerosal on Ca^{2+} release provoked by 200 nM IP$_3$ in the presence of 1 μM free Ca^{2+}. (**C**) Bell-shaped dependence of the effect of thimerosal on IICR. Data are plotted as the difference between the fractional loss after the addition of IP$_3$ and the fractional loss before the addition of IP$_3$ as a function of the thimerosal concentration: $\bigcirc$, 200 nM IP$_3$, 1 mM EGTA; $\square$, 200 nM IP$_3$, 1 μM free Ca^{2+}; $\triangle$, 750 nM IP$_3$, 1 mM EGTA. (**D**) Effect of NEM ($\bigcirc$), diamide ($\square$) and SIN-1 ($\triangle$) on IICR. Data are plotted as the difference between the fractional loss after the addition of IP$_3$ and the fractional loss before the addition of IP$_3$ as a function of the NEM, diamide or SIN-1 concentration respectively. The experiment was performed using 750 nM IP$_3$ and in the presence of 1 mM EGTA. Each curve represents the means $\pm$ S.E.M for three wells.

bell-shaped dependence on the thimerosal concentration was observed, but the maximum depended on the presence of Ca^{2+} (Figure 4C). In the absence of Ca^{2+}, the maximum stimulation was reached with between 3 and 10 μM thimerosal, whereas in the presence of 1 μM free Ca^{2+}, the maximum was obtained at 1 μM thimerosal. The shift to lower concentrations of thimerosal was not due to the higher Ca^{2+}-release activity in the presence of Ca^{2+}, since in the absence of Ca^{2+}, but using 750 nM IP$_3$ to evoke Ca^{2+} release, maximum stimulation was still reached with between 3 and 10 μM thimerosal. The additive effect of thimerosal and Ca^{2+} on the activation of IICR may indicate that both agents co-operate to induce a conformation that is much more sensitive towards activation by IP$_3$.

Other agents that interact with cysteine residues could not mimic the effect of thimerosal. NEM did not affect IICR, indicating that alkylation of cysteine residues is insufficient (Figure 4D). The NO donor SIN-1, capable of nitrosylation of cysteine residues, also had no effect on IICR, whereas diamide, which is known to cross-link disulphide bridges of cysteine residues, had an inhibitory effect on IICR.

Interaction of the N-terminal 225 amino acids with the IP$_3$-binding core (amino acids 226–604)

Since the N-terminal 225 amino acids seemed to be critical for the effect of thimerosal on IP$_3$ binding (Figure 3A), we investigated the role of this domain in thimerosal-dependent intramolecular in-
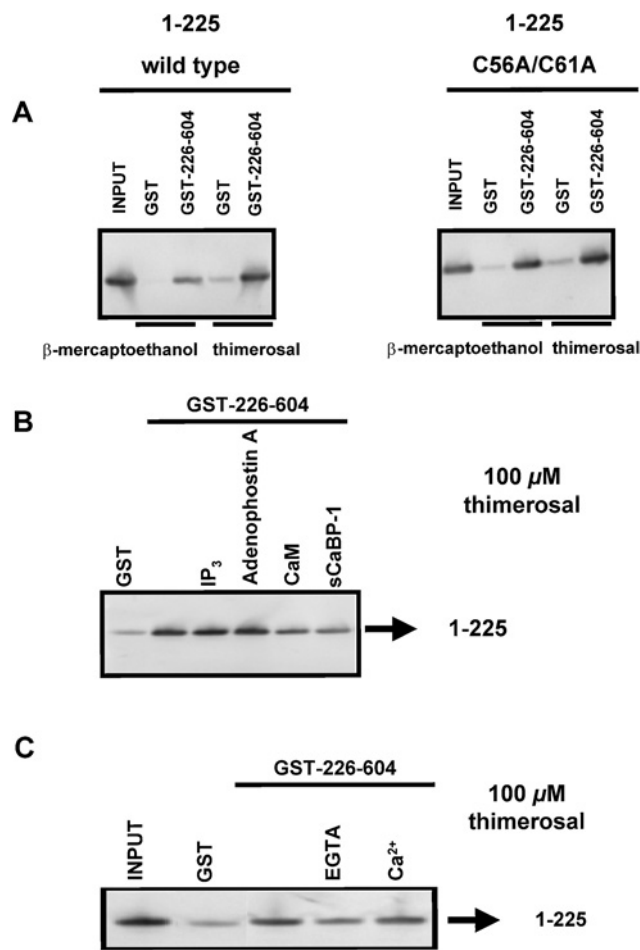

Figure 5   Interaction between amino acids 1–225 and 226–604 of IP$_3$R1

(**A**) Pull-down experiment applied for GST–226–604 with 1–225 wild-type and with 1–225 C56A/C61A in the presence of 1 mM 2-mercaptoethanol or 100 μM thimerosal. C56 and C61, two conserved cysteine residues in the suppressor domain, were mutated into alanine residues. The recombinant suppressor domains were incubated with GST or GST–226–604 immobilized on glutathione–Sepharose 4B. After washing, the retained proteins were eluted. After SDS/PAGE, the proteins were analysed by immunoblotting with the anti-IP$_3$R polyclonal antibody Rbt475. Input (1–225 protein) was always 50 ng, whereas the lanes representing samples obtained after GST-pull down contained 2.5-fold more material. (**B**) Pull-down experiment applied for GST–226–604 with 1–225 in the presence of 100 μM thimerosal. The experimental procedure was the same as that described in (**A**). During the incubation reaction, 25 μM IP$_3$, 25 μM adenophostin A, 10 μM CaM or 10 μM sCaBP-1 was added. CaM and sCaBP-1 significantly inhibited the interaction to 44 $\pm$ 13 and 37 $\pm$ 12 % of the control respectively. (**C**) Pull-down experiment applied for GST–226–604 with 1–225 in the presence or absence of Ca^{2+}. Thimerosal (100 μM) was added during the incubation step. The experimental procedure was the same as that described in (**A**). The absence of Ca^{2+} inhibited the interaction to 26 $\pm$ 18 % of the control. Results are the means $\pm$ S.D. for at least three independent experiments.

teractions. IP$_3$-binding cores (amino acids 226–604) of both IP$_3$R1 and IP$_3$R3 were immobilized as GST fusion proteins on gluta-thione–Sepharose 4B. The suppressor domains (amino acids 1–225) of IP$_3$R1 and IP$_3$R3 were obtained from GST fusion proteins by proteolytic cleavage. Western-blot analysis using the Rbt475 antibody revealed that these 1–225 fragments were ex-pressed as stable proteins and migrated in gels as single bands (results not shown). Under reducing conditions (1 mM 2-mercaptoethanol), we found that the suppressor domain of IP$_3$R1 specifically interacted with the IP$_3$-binding core of IP$_3$R1 (Fig-ure 5A, left panel). The binding was relatively weak, since only 5 $\pm$ 2 % ($n = 4$ independent experiments) of the 1–225 fragments was retained by immobilized GST–226–604 (Table 2). In the

Table 2   Specific binding of 1–225 type 1 or 3 to immobilized GST–226–604 type 1 or 3 in the presence of 2-mercaptoethanol, NEM or thimerosal

Purified 1–225 proteins were incubated with immobilized GST–226–604 fusion proteins in their respective interaction buffer, containing 2-mercaptoethanol (1 mM), NEM (300 μM) or thimerosal (100 μM). After washing and elution, the proteins (the equivalent of 125 or 200 ng) were separated on NuPAGE® 4–12 % Bis-Tris gels and analysed by Western blotting using Rbt475 (1:3000). Immunoreactive bands were quantified by using ImageQuant 5.2 software and the binding efficiency was calculated against 50 ng of input protein (%). Specific binding was determined by subtracting the binding to immobilized GST in the presence of 2-mercaptoethanol, NEM or thimerosal. Results are the means $\pm$ S.D. for at least four independent experiments. Abbreviation: NS, not significant.

	Specific binding (%) (means $\pm$ S.D.)	
	GST–226–604 IP$_3$R1	GST–226–604 IP$_3$R3
1–225 protein IP$_3$R1		
2-Mercaptoethanol	5 ± 2	NS
NEM	7 ± 2	NS
Thimerosal	33 ± 6	6 ± 2
1–225 protein IP$_3$R3		
2-Mercaptoethanol	NS	NS
NEM	NS	NS
Thimerosal	$4 \pm 2\%$	NS

presence of 100 μM thimerosal, the binding efficiency was increased approx. 6-fold, and up to 33 ± 6 % ($n = 4$) of the input was retained on the column (Figure 5A, left panel). In the presence of 300 μM NEM, we could not detect any significant increase in the binding efficiency (Table 2).

The effect of thimerosal on the intramolecular interaction appeared to be specific for IP$_3$R1. The 1–225 fragment of IP$_3$R3 did not interact with immobilized GST–226–604 protein of IP$_3$R3 in the presence of 2-mercaptoethanol. Neither NEM nor thimerosal could induce a significant interaction (Table 2).

We also investigated the cross-interaction between types 1 and 3 by incubating the 1–225 fragment of IP$_3$R1 with immobilized GST–226–604 of IP$_3$R3 and vice versa. No significant interactions were observed and neither NEM nor thimerosal could stimulate domain interactions (Table 2). When we mutated the two cysteine residues conserved in all isoforms, i.e. at positions 56 and 61 of mouse IP$_3$R1, into alanine residues, we found that thimerosal was still capable of stimulating this interaction to the same extent as the wild-type (Figure 5A, right panel). In addition, the full-size IP$_3$R1 carrying those mutations was stimulated by thimerosal to the same extent as the wild-type IP$_3$R1 (results not shown). This result suggests that thimerosal interacts with IP$_3$R1 via non-conserved cysteine residues.

IP$_3$, adenophostin A, CaM (calmodulin) and sCaBP-1 (short Ca^{2+}-binding protein-1) interact within the first 604 amino acids of mouse IP$_3$R1. In the presence of 2-mercaptoethanol, none of these compounds and none of these proteins modulated the interaction between the suppressor and IP$_3$-binding core of IP$_3$R1 (results not shown). However, the thimerosal-dependent interaction was significantly inhibited by CaM and sCaBP-1 to approx. 44 ± 13 and 37 ± 12 % of the control conditions respectively ($n = 4$ and $P < 0.01$; P value obtained by paired Student's t test of the significantly different conditions; Figure 5B), whereas IP$_3$ and adenophostin A did not have any effect on the binding efficiency (Figure 5B).

Since the effect of thimerosal on IICR via IP$_3$R1 appeared to depend on Ca^{2+}, we also investigated whether Ca^{2+} modulated the effect of thimerosal on the interaction between the suppressor and IP$_3$-binding core of IP$_3$R1. When Ca^{2+} was removed from

the incubation buffer by the addition of 1 mM EGTA, the binding efficiency was indeed reduced to approx. 26 ± 18 % ($n = 3$ and $P < 0.01$) of the control conditions, which was done at nominal [Ca^{2+}] (Figure 5C). However, addition of 25 μM Ca^{2+} did not significantly alter the binding efficiency.

Effects of thimerosal and IP$_3$ on the interaction of the IP$_3$-binding and transmembrane domains

A weak interaction between ligand-binding and transmembrane domains has been described in homo- and hetero-tetrameric IP$_3$Rs [31]. In the C-terminal tail, there are two highly conserved cysteine residues (Cys-2610 and Cys-2613) that appear to be essential for channel opening [5]. In addition, a C-terminal monoclonal antibody was shown to inhibit Ca^{2+} oscillations and thimerosal-induced sensitization of IICR [32]. Therefore we decided to characterize the effects of thimerosal and Ca^{2+} on the interaction between the IP$_3$-binding and transmembrane domains. The IP$_3$-binding domain of IP$_3$R1 (amino acids 1–604) was expressed as a GST fusion protein (GST–1–604) and a pull-down assay was applied for the C-terminal transmembrane domain of IP$_3$R1 (amino acids 2170–2749) tagged with three adjacent FLAG epitopes [FLAG(2170–2749)]. FLAG(2170–2749) was expressed in COS-1 cells and the microsomes were lysed in a Triton X-100-containing buffer. The N- and C-terminal association was confirmed as shown in Figure 6(A). Thimerosal (100 μM) or Ca^{2+} (25 μM) alone or a combination of both the compounds could not alter this interaction between the N- and C-terminal domains. The double band of the FLAG(2170–2749) is due to partial glycosylation of this protein. In contrast with previous findings [31], we found that 20 μM IP$_3$ or adenophostin A significantly weakened the interaction (Figure 6B). For IP$_3$, 45 ± 5 % ($n = 3$ and $P < 0.05$) of the control (without IP$_3$) FLAG(2170–2749) was retained on the column. Adenophostin A had even a stronger effect, since only 32 ± 8 % ($n = 3$ and $P < 0.05$) compared with the control condition was retained by GST–1–604. This discrepancy between our results and results of previous studies is probably due to different experimental approaches.

DISCUSSION

In the present study, we have analysed the effects of the thiol-reactive agent thimerosal, which is a well-known activator of IP$_3$R capable of inducing Ca^{2+} oscillations in a number of cells [32,33]. The effect of thimerosal has been linked to an increase in the affinity of IP$_3$Rs for IP$_3$ [17,18,34] and an increase in channel conductance and mean opening time [35]. Effects of thimerosal appear to be dependent on the redox state of the receptor, implying a direct action of thimerosal on one or more critical thiol groups [17]. However, the molecular mechanism and identity of these critical cysteine residues on IP$_3$R are still not known. Thimerosal has been shown to lower significantly the threshold for IP$_3$ action [36], whereas it only moderately enhances IP$_3$ binding. Therefore it is conceivable that thimerosal interferes with conformational changes of IP$_3$R that are crucial for activation.

The IP$_3$-binding domain of IP$_3$R1 is composed of two different functional and structural parts: an N-terminal 225-amino-acid fragment and a succeeding 351-residue-fragment (amino acids 226–576), which forms the IP$_3$-binding core [37,38]. The affinity for IP$_3$ of this IP$_3$-binding core is more than 10-fold higher compared with that of the full IP$_3$-binding domain [37]. In addition, it was shown that the first 225-amino-acid fragment is critical for IP$_3$R gating [5]. This domain was therefore referred to as a coupling/suppressor domain. In the present study, we describe a novel association between the coupling/suppressor domain and
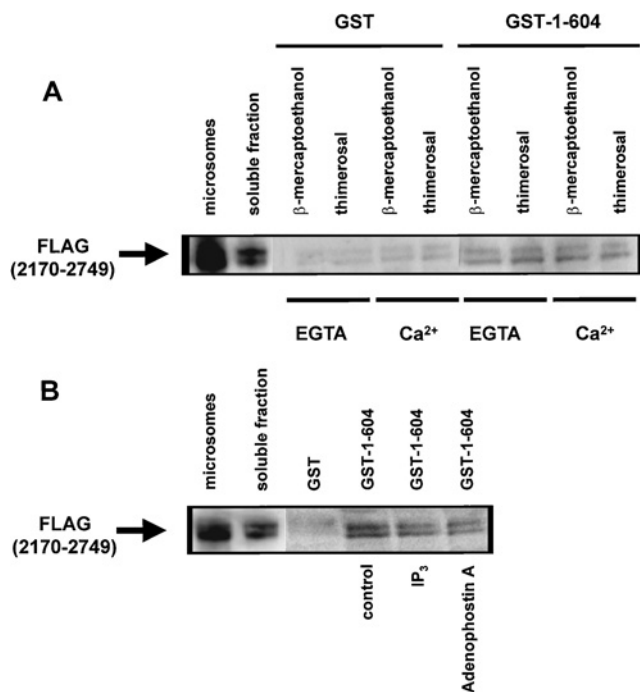
Figure 6   Effect of thimerosal and IP$_3$ on the interaction between the IP$_3$-binding and transmembrane domains of IP$_3$R1

(**A**) Pull-down experiment applied for GST–1–604 with FLAG(2170–2749) in the presence of 1 mM 2-mercaptoethanol or 100 μM thimerosal. EGTA (1 mM) or 25 μM Ca^{2+} was added as indicated in the Figure. The recombinant FLAG(2170–2749) was incubated with GST or GST–1–604 immobilized on glutathione–Sepharose 4B. After washing, the retained proteins were eluted. After SDS/PAGE, the proteins were analysed by immunoblotting with ANTI-FLAG® M2 monoclonal antibody. Lane 'microsomes' contains 0.5 μg of protein and lane 'soluble fraction' contains 2 μg of protein, whereas the lanes representing samples obtained after GST-pull down contain 15-fold more material than the soluble fraction. (**B**) Pull-down experiment applied for GST–1–604 with FLAG(2170–2749) in the presence of 1 mM 2-mercaptoethanol. During the incubation reaction, 20 μM IP$_3$ or adenophostin A was added. The experimental procedure was the same as that described in (**A**). IP$_3$ and adenophostin A significantly inhibited the interaction to 45 $\pm$ 5 and 32 $\pm$ 8 % of the control respectively. Results are the means $\pm$ S.D. for at least three independent experiments.

the IP$_3$-binding core is described that was enhanced by both thimerosal and Ca^{2+}. Accordingly, we observed that the previously demonstrated bell-shaped dependence of IICR on thimerosal in A7r5 cells [16] shifted to lower thimerosal concentrations in the presence of Ca^{2+}. This analogy between the molecular data on the one hand and the functional experiments in A7r5 cells on the other allows us to conclude that Ca^{2+} and thimerosal co-operate to render IP$_3$R1 more sensitive to IP$_3$ and the interaction between the coupling/suppressor domain and the IP$_3$-binding core is probably the molecular basis for this sensitization. This is compatible with experiments in hamster eggs, where it was also shown that both thimerosal and Ca^{2+} synergetically sensitize IICR [32]. This effect was isoform-specific. In agreement with the lack of effect of thimerosal on IP$_3$R3 [19–21], we found that thimerosal did not enhance the interaction between the coupling/suppressor domain and the IP$_3$-binding core of IP$_3$R3. Also, in R23-11 cells stably expressing IP$_3$R3, thimerosal could not affect IICR or IP$_3$ binding.

The main question remains as to how changes in intramolecular interactions of the N-terminal part of the receptor are translated into altered Ca^{2+}-flux properties of the C-terminal part of the receptor. Since it was suggested that the two conserved residues in the C-terminus (Cys-2610 and Cys-2613) could be the targets of thiol reagents [32], we investigated whether thimerosal might

alter the interaction between the N- and C-terminal domains. However, we did not detect any thimerosal-dependent interaction between the N- and C-termini either in the presence or absence of Ca^{2+}. Therefore the stimulatory action of thimerosal appears to be related solely to conformational changes in the N-terminal region of the receptor. These changes may be sensed by the C-terminal channel domain via the N-terminal coupling/suppressor domain [5], thereby enhancing the opening of the channel pore. Support for this view comes from the observation that, for IP$_3$R3, the N-terminal intramolecular interaction and its modulation by thimerosal are completely absent, in agreement with the lack of stimulation of IP$_3$R3 by thimerosal. The thimerosal-dependent N-terminal interaction in IP$_3$R1 was inhibited by CaM and by CaM-like sCaBP-1. Both proteins interact specifically within the N-terminal domain of IP$_3$Rs [39–41]. CaM inhibited IICR and IP$_3$ binding [42,43], whereas sCaBP-1 was found to stimulate [40] or to inhibit [41,44] Ca^{2+} release. It is conceivable that CaM and sCaBP-1 exert their effects by disrupting the intramolecular interaction in the N-terminal region, which is required for activation of the channel and the increase in function by thimerosal. A similar situation is found for ryanodine receptor 1, where the activation by NO is dependent on endogenous CaM and antagonizes the inhibition by CaM without displacing it from the channel. Mutation of conserved Cys-3635, which is located in or near the CaM-binding domain of ryanodine receptor 1, resulted in the loss of CaM-dependent NO modulation and reduced S-nitrosylation by NO [45,46].

Although neither thimerosal nor Ca^{2+} modulated the interaction between the N-terminal IP$_3$-binding and C-terminal transmembrane domains of IP$_3$R1, we observed that IP$_3$ and adenophostin A clearly weakened it. This may indicate that the N-terminal IP$_3$-binding domain prevents unco-ordinated opening and activation of the channel in the absence of the ligand. When occupied by IP$_3$ or adenophostin A, the affinity of the IP$_3$-binding domain for the C-terminus decreases and this may allow proper opening of the channel pore. This IP$_3$-sensitive link between the N- and C-terminal parts of the receptor may be a part of the mechanism for IP$_3$-induced activation of the channel.

Although we cannot exclude the possibility that thimerosal may also affect other intramolecular interactions in the structure of IP$_3$R1 that participate in coupling IP$_3$ binding to channel domain, our results clearly show that the interaction of thimerosal with the N-terminal domain of IP$_3$R1 is functionally important and enhances Ca^{2+} flux via conformational changes involving the N-terminal coupling domain. It is tempting to suggest that the windmill-like structure of the receptor that is achieved in the presence of Ca^{2+} [14,15] is more accessible for thimerosal. This would explain the synergetic effect of Ca^{2+} and thimerosal on IP$_3$R1.

Our results also show that the oxidizing effect of thimerosal is specific and cannot be mimicked by the addition of NEM or diamide. We cannot exclude that these thiol-modifying agents act on cysteine residues other than that in thimerosal. Thimerosal exerts a biphasic effect: the stimulatory effect of thimerosal is only observed at lower concentrations, whereas higher concentrations have inhibitory effects on Ca^{2+} release and IP$_3$ binding. This suggests that thimerosal may exert a specific action on a limited number of cysteine residues in the N-terminal part of IP$_3$R1 at lower thimerosal concentrations, whereas it may affect other cysteine residues at high concentrations and thereby abolish the Ca^{2+}-flux properties of the channel. Poirier et al. [47] have pointed out that the conformational state adopted by IP$_3$R after a drastic treatment with a thiol-reactive agent is irreversible and corresponds to a non-binding state. This may explain the bell-shaped dependence of IICR on thimerosal and the finding that diamide inhibits Ca^{2+} flux in a dose-dependent manner. Mutational analysis of the

different cysteine residues in the IP$_3$R1 constructs may reveal the critical component responsible for the thimerosal- and Ca^{2+}-induced 'gain of function' process. At a later stage it will be necessary to evaluate different physiological agents that could mimic the effects of thimerosal on the intramolecular interaction and on the Ca^{2+}-flux properties of IP$_3$R1. The reactive oxygen species that are produced during different physiological processes may be good candidates.

Taken together, our results revealed a thimerosal-dependent intramolecular interaction within the N-terminal domain of IP$_3$R1. This interaction is Ca^{2+}-dependent and isoform-specific. These properties are entirely compatible with functional observations on IICR showing that thimerosal stimulation was potentiated in the presence of Ca^{2+} and the stimulatory effect of thimerosal was isoform-specific. This intramolecular interaction may therefore be responsible for at least a part of the conformational changes occurring during the sensitization of IP$_3$R1 by thimerosal. In addition, IP$_3$ may induce the opening of the channel pore by modifying the interaction of the C-terminal channel domain with the N-terminal IP$_3$-binding domain.

REFERENCES

1 Berridge, M. J. (1993) Inositol trisphosphate and calcium signalling. Nature (London) **361**, 315–325

2 Furuichi, T. and Mikoshiba, K. (1995) Inositol 1,4,5-trisphosphate receptor-mediated Ca^{2+} signaling in the brain. J. Neurochem. **64**, 953–960

3 Südhof, T. C., Newton, C. L., Archer, B. T. D., Ushkaryov, Y. A. and Mignery, G. A. (1991) Structure of a novel InsP$_3$ receptor. EMBO J. **10**, 3199–3206

4 Yoshikawa, F., Iwasaki, H., Michikawa, T., Furuichi, T. and Mikoshiba, K. (1999) Trypsinized cerebellar inositol 1,4,5-trisphosphate receptor. Structural and functional coupling of cleaved ligand binding and channel domains. J. Biol. Chem. **274**, 316–327

5 Uchida, K., Miyauchi, H., Furuichi, T., Michikawa, T. and Mikoshiba, K. (2003) Critical regions for activation gating of the inositol 1,4,5-trisphosphate receptor. J. Biol. Chem. **278**, 16551–16560

6 Iino, M. (1990) Biphasic Ca^{2+} dependence of inositol 1,4,5-trisphosphate-induced Ca^{2+} release in smooth muscle cells of the guinea pig *Taenia caeci*. J. Gen. Physiol. **95**, 1103–1122

7 Bezprozvanny, I., Watras, J. and Ehrlich, B. E. (1991) Bell-shaped calcium-response curves of Ins(1,4,5)P$_3$- and calcium-gated channels from endoplasmic reticulum of cerebellum. Nature (London) **351**, 751–754

8 Parys, J. B., Sernett, S. W., DeLisle, S., Snyder, P. M., Welsh, M. J. and Campbell, K. P. (1992) Isolation, characterization, and localization of the inositol 1,4,5-trisphosphate receptor protein in *Xenopus laevis* oocytes. J. Biol. Chem. **267**, 18776–18782

9 Marshall, I. C. and Taylor, C. W. (1993) Biphasic effects of cytosolic Ca^{2+} on Ins(1,4,5)P$_3$-stimulated Ca^{2+} mobilization in hepatocytes. J. Biol. Chem. **268**, 13214–13220

10 Sienaert, I., De Smedt, H., Parys, J. B., Missiaen, L., Vanlingen, S., Sipma, H. and Casteels, R. (1996) Characterization of a cytosolic and a luminal Ca^{2+} binding site in the type I inositol 1,4,5-trisphosphate receptor. J. Biol. Chem. **271**, 27005–27012

11 Sienaert, I., Missiaen, L., De Smedt, H., Parys, J. B., Sipma, H. and Casteels, R. (1997) Molecular and functional evidence for multiple Ca^{2+}-binding domains in the type 1 inositol 1,4,5-trisphosphate receptor. J. Biol. Chem. **272**, 25899–25906

12 Miyakawa, T., Mizushima, A., Hirose, K., Yamazawa, T., Bezprozvanny, I., Kurosaki, T. and Iino, M. (2001) Ca^{2+}-sensor region of IP$_3$ receptor controls intracellular Ca^{2+} signaling. EMBO J. **20**, 1674–1680

13 Tu, H., Nosyreva, E., Miyakawa, T., Wang, Z., Mizushima, A., Iino, M. and Bezprozvanny, I. (2003) Functional and biochemical analysis of the type 1 inositol (1,4,5)-trisphosphate receptor calcium sensor. Biophys. J. **85**, 290–299

14 Hamada, K., Miyata, T., Mayanagi, K., Hirota, J. and Mikoshiba, K. (2002) Two-state conformational changes in inositol 1,4,5-trisphosphate receptor regulated by calcium. J. Biol. Chem. **277**, 21115–21118

15 Hamada, K., Terauchi, A. and Mikoshiba, K. (2003) Three-dimensional rearrangements within inositol 1,4,5-trisphosphate receptor by calcium. J. Biol. Chem. **278**, 52881–52889

16 Parys, J. B., Missiaen, L., De Smedt, H., Droogmans, G. and Casteels, R. (1993) Bell-shaped activation of inositol-1,4,5-trisphosphate-induced Ca^{2+} release by thimerosal in permeabilized A7r5 smooth-muscle cells. Pflügers Arch. **424**, 516–522

17 Kaplin, A. I., Ferris, C. D., Voglmaier, S. M. and Snyder, S. H. (1994) Purified reconstituted inositol 1,4,5-trisphosphate receptors. Thiol reagents act directly on receptor protein. J. Biol. Chem. **269**, 28972–28978

18 Missiaen, L., Taylor, C. W. and Berridge, M. J. (1992) Luminal Ca^{2+} promoting spontaneous Ca^{2+} release from inositol trisphosphate-sensitive stores in rat hepatocytes. J. Physiol. (Cambridge, U.K.) **455**, 623–640

19 Missiaen, L., Parys, J. B., Sienaert, I., Maes, K., Kunzelmann, K., Takahashi, M., Tanzawa, K. and De Smedt, H. (1998) Functional properties of the type-3 InsP$_3$ receptor in 16HBE14o-bronchial mucosal cells. J. Biol. Chem. **273**, 8983–8986

20 Vanlingen, S., Sipma, H., Missiaen, L., De Smedt, H., De Smet, P., Casteels, R. and Parys, J. B. (1999) Modulation of type 1, 2 and 3 inositol 1,4,5-trisphosphate receptors by cyclic ADP-ribose and thimerosal. Cell Calcium **25**, 107–114

21 Vanlingen, S., Sipma, H., De Smet, P., Callewaert, G., Missiaen, L., De Smedt, H. and Parys, J. B. (2001) Modulation of inositol 1,4,5-trisphosphate binding to the various inositol 1,4,5-trisphosphate receptor isoforms by thimerosal and cyclic ADP-ribose. Biochem. Pharmacol. **61**, 803–809

22 Miyakawa, T., Maeda, A., Yamazawa, T., Hirose, K., Kurosaki, T. and Iino, M. (1999) Encoding of Ca^{2+} signals by differential expression of IP$_3$ receptor subtypes. EMBO J. **18**, 1303–1308

23 Parys, J. B., De Smedt, H. and Borghgraef, R. (1986) Calcium transport systems in the LLC-PK1 renal epithelial established cell line. Biochim. Biophys. Acta **888**, 70–81

24 Lowry, O. H., Rosebrough, N. J., Farr, A. L. and Randall, R. F. (1951) Protein measurement with the Folin phenol reagent. J. Biol. Chem. **193**, 265–275

25 Sipma, H., De Smet, P., Sienaert, I., Vanlingen, S., Missiaen, L., Parys, J. B. and De Smedt, H. (1999) Modulation of inositol 1,4,5-trisphosphate binding to the recombinant ligand-binding site of the type-1 inositol 1,4,5-trisphosphate receptor by Ca^{2+} and calmodulin. J. Biol. Chem. **274**, 12157–12162

26 Ma, H. T., Venkatachalam, K., Parys, J. B. and Gill, D. L. (2002) Modification of store-operated channel coupling and inositol trisphosphate receptor function by 2-aminoethoxydiphenyl borate in DT40 lymphocytes. J. Biol. Chem. **277**, 6915–6922

27 Parys, J. B., De Smedt, H., Missiaen, L., Bootman, M. D., Sienaert, I. and Casteels, R. (1995) Rat basophilic leukemia cells as model system for inositol 1,4,5-trisphosphate receptor IV, a receptor of the type II family: functional comparison and immunological detection. Cell Calcium **17**, 239–249

28 Grynkiewicz, G., Poenie, M. and Tsien, R. Y. (1985) A new generation of Ca^{2+} indicators with greatly improved fluorescence properties. J. Biol. Chem. **260**, 3440–3450

29 Missiaen, L., Taylor, C. W. and Berridge, M. J. (1991) Spontaneous calcium release from inositol trisphosphate-sensitive calcium stores. Nature (London) **352**, 241–244

30 Nadif Kasri, N., Sienaert, I., Parys, J. B., Callewaert, G., Missiaen, L., Jeromin, A. and De Smedt, H. (2003) A novel Ca^{2+}-induced Ca^{2+} release mechanism in A7r5 cells regulated by calmodulin-like proteins. J. Biol. Chem. **278**, 27548–27555

31 Boehning, D. and Joseph, S. K. (2000) Direct association of ligand-binding and pore domains in homo- and heterotetrameric inositol 1,4,5-trisphosphate receptors. EMBO J. **19**, 5450–5459

32 Miyazaki, S., Shirakawa, H., Nakada, K., Honda, Y., Yuzaki, M., Nakade, S. and Mikoshiba, K. (1992) Antibody to the inositol trisphosphate receptor blocks thimerosal-enhanced Ca^{2+}-induced Ca^{2+} release and Ca^{2+} oscillations in hamster eggs. FEBS Lett. **309**, 180–184

33 Bootman, M. D., Taylor, C. W. and Berridge, M. J. (1992) The thiol reagent, thimerosal, evokes Ca^{2+} spikes in HeLa cells by sensitizing the inositol 1,4,5-trisphosphate receptor. J. Biol. Chem. **267**, 25113–25119

34 Hilly, M., Pietri Rouxel, F., Coquil, J. F., Guy, M. and Mauger, J. P. (1993) Thiol reagents increase the affinity of the inositol 1,4,5-trisphosphate receptor. J. Biol. Chem. **268**, 16488–16494

35 Thrower, E. C., Duclohier, H., Lea, E. J., Molle, G. and Dawson, A. P. (1996) The inositol 1,4,5-trisphosphate-gated Ca^{2+} channel: effect of the protein thiol reagent thimerosal on channel activity. Biochem. J. **318**, 61–66

36 Missiaen, L., De Smedt, H., Parys, J. B., Sienaert, I., Vanlingen, S. and Casteels, R. (1996) Threshold for inositol 1,4,5-trisphosphate action. J. Biol. Chem. **271**, 12287–12293

37 Yoshikawa, F., Morita, M., Monkawa, T., Michikawa, T., Furuichi, T. and Mikoshiba, K. (1996) Mutational analysis of the ligand binding site of the inositol 1,4,5-trisphosphate receptor. J. Biol. Chem. **271**, 18277–18284

38 Bosanac, I., Alattia, J. R., Mal, T. K., Chan, J., Talarico, S., Tong, F. K., Tong, K. I., Yoshikawa, F., Furuichi, T., Iwai, M. et al. (2002) Structure of the inositol 1,4,5-trisphosphate receptor binding core in complex with its ligand. Nature (London) **420**, 696–700

39 Sienaert, I., Nadif Kasri, N., Vanlingen, S., Parys, J. B., Callewaert, G., Missiaen, L. and De Smedt, H. (2002) Localization and function of a calmodulin-apocalmodulin-binding domain in the N-terminal part of the type 1 inositol 1,4,5-trisphosphate receptor. Biochem. J. **365**, 269–277

40 Yang, J., McBride, S., Mak, D. O., Vardi, N., Palczewski, K., Haeseleer, F. and Foskett, J. K. (2002) Identification of a family of calcium sensors as protein ligands of inositol trisphosphate receptor Ca^{2+} release channels. Proc. Natl. Acad. Sci. U.S.A. **99**, 7711–7716

41 Nadif Kasri, N., Holmes, A. M., Bultynck, G., Parys, J. B., Bootman, M. D., Rietdorf, K., Missiaen, L., McDonald, F., De Smedt, H., Conway, S. J. et al. (2004) Regulation of $InsP_3$ receptor activity by neuronal Ca^{2+}-binding proteins. EMBO J. **23**, 312–321

42 Nadif Kasri, N., Bultynck, G., Sienaert, I., Callewaert, G., Erneux, C., Missiaen, L., Parys, J. B. and De Smedt, H. (2002) The role of calmodulin for inositol 1,4,5-trisphosphate receptor function. Biochim. Biophys. Acta **1600**, 19–31

43 Taylor, C. W. and Laude, A. J. (2002) IP_3 receptors and their regulation by calmodulin and cytosolic Ca^{2+}. Cell Calcium **32**, 321–334

44 Haynes, L. P., Tepikin, A. V. and Burgoyne, R. D. (2003) Calcium binding protein 1 is an inhibitor of agonist-evoked, inositol 1,4,5-trisphosphate-mediated calcium signalling. J. Biol. Chem. **279**, 547–555

45 Eu, J. P., Sun, J., Xu, L., Stamler, J. S. and Meissner, G. (2000) The skeletal muscle calcium release channel: coupled O_2 sensor and NO signaling functions. Cell (Cambridge, Mass.) **102**, 499–509

46 Sun, J., Xin, C., Eu, J. P., Stamler, J. S. and Meissner, G. (2001) Cysteine-3635 is responsible for skeletal muscle ryanodine receptor modulation by NO. Proc. Natl. Acad. Sci. U.S.A. **98**, 11158–11162

47 Poirier, S. N., Poitras, M., Laflamme, K. and Guillemette, G. (2001) Thiol-reactive agents biphasically regulate inositol 1,4,5-trisphosphate binding and Ca^{2+} release activities in bovine adrenal cortex microsomes. Endocrinology **142**, 2614–2621